

# 5-Bit Programmable Binary and Ternary Architectures for an Optical Transmit/Receive Beamformer

Sabarni PALIT<sup>†</sup>, Mark JAEGER<sup>††</sup>, Sergio GRANIERI<sup>††</sup>, Azad SIAHMAKOUN<sup>††a)</sup>, Bruce BLACK<sup>†</sup>, and Jeffrey CHESTNUT<sup>†††</sup>, *Nonmembers*

**SUMMARY** Binary and ternary 5-bit programmable dispersion matrix, based on fiber Bragg reflectors, is built to control a two-channel receive/transmit beamformer at 1550 nm. RF phase measurements for the 32/31 delay configurations are presented. The programmable dispersion matrix is fully demonstrated and characterized for RF signals from 0.2 to 1 GHz.

**key words:** optical signal processing, phased-array antennas, fiber Bragg gratings, true-time delay beamforming

## 1. Introduction

Many RF and microwave systems, such as high-resolution phased-array antennas and signal processing electronics, require true-time delay (TTD) phase shifters. In such systems, the individual T/R-element control allows the implementation of beam steering and shaping. In conventional RF systems, TTD is achieved by switching to different lengths of electrical cable. However, these implementations tend to be bulky, heavy and susceptible to electromagnetic interference. The fiber-optic control systems provide benefits in the above areas.

Varieties of optical techniques have been proposed for obtaining TTD capability using fiber-optic systems [1]. In particular, systems using fiber Bragg reflectors for providing time delays have been proposed and demonstrated [2], [3]. In Ref. [4] a 2-bit transmit/receive module using a fiber Bragg grating matrix has been demonstrated.

In this paper, we design and experimentally demonstrate a binary and ternary version of a two-channel true-time delay programmable dispersion matrix (PDM) for controlling a phase array antenna. The wideband processor has a resolution of 5-bit and it can be easily scaled to large number of T/R elements.

In Sect. 2 we describe in detail the theory for both architectures along with an overview of the beamformer

in transmit and receive modes. The beamformer measurements and analysis are discussed in Sect. 3. Concluding remarks are given in Sect. 4.

## 2. System Overview

Figure 1(a) shows a schematic drawing of the beamformer architecture in the transmit mode. Two laser diodes provide optical carriers (channels) with wavelength  $\lambda_1$  and  $\lambda_2$ . Both channels are multiplexed and externally modulated with an RF signal using a Mach-Zehnder electro-optic modulator (EOM). Modulation of multiplexed channels ensures zero phase delay between the RF components before the optical carrier is processed in transmit mode. Modulated carriers feed a

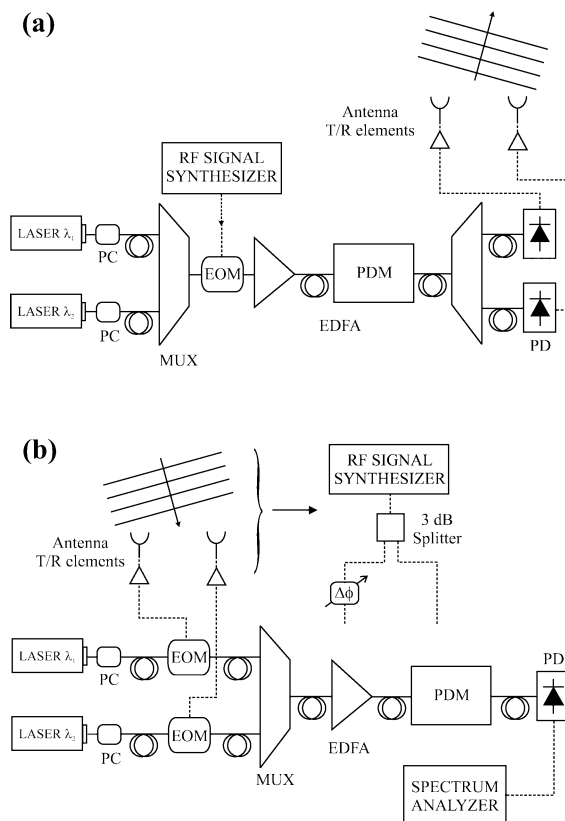


**Fig. 1** Beamformer setup configuration for: (a) transmit mode and (b) receive mode. PC: polarization controller, PD: photodiode.

Manuscript received November 29, 2002.

Manuscript revised January 29, 2003.

<sup>†</sup>The authors are with the Department of Electrical Engineering, Rose-Hulman Institute of Technology, 5500 Wabash Ave., Terre Haute, Indiana 47803, USA.

<sup>††</sup>The authors are with the Department of Physics and Optical Engineering, Rose-Hulman Institute of Technology, 5500 Wabash Ave., Terre Haute, Indiana 47803, USA.

<sup>†††</sup>The author is with NSWC-Crane Division, 300 Highway 361, Crane, Indiana 47522, USA.

a) E-mail: siahmakoun@rose-hulman.edu

PDM, which performs the true-time delay processing. For each configuration of the PDM,  $\lambda_1$  either leads or lags  $\lambda_2$  by a time-period. At the output of the PDM, after proper phase difference is set, channels are demultiplexed. Two broadband photo-detectors recover the delayed RF signals that would feed the antenna elements.

The schematic drawing for a receive-mode beamformer is shown in Fig. 1(b). An incoming RF signal from a target is received by the two antenna array elements. The phase difference at the antenna elements depends on the target position. The received RF signal at each element separately modulates two individual optical carriers, at wavelengths  $\lambda_1$  and  $\lambda_2$ .

Modulation of optical carriers is performed by two Mach-Zehnder EOMs. The multiplexed optical carriers feed the PDM, which performs the true-time delay processing. The time delay between optical channels is corrected by the PDM and detected with a single photodetector. The output power of the photodetector is a function of the corrected phase difference between the two RF signals and is given by

$$P \text{ (dB)} = 10 \log (K_1 + K_2 \cos \Delta\phi) \quad (1)$$

where  $\Delta\phi$  is the phase difference and  $K_1$ ,  $K_2$  are the proportionality constants. Thus, the output power is related to the target angular position via this phase difference. When the PDM corrects for the phase difference at the antenna elements a maximum power will be detected for the target position.

## 2.1 PDM Binary and Ternary Architectures

The architecture of a binary 5-bit PMD, which is based on fiber Bragg grating (FBG) arrays, is shown in Fig. 2(a). The  $N$ -bit version of two-channel binary architecture consists of an array of  $N$  delay lines. Each delay line is constructed by splicing two FBGs. The center wavelength of each FBG matches the wavelengths of the multiplexed optical channels. The separation between Bragg reflectors is different for each delay line. Thus, the time delay(s) between channels are proportional to these FBG separations. The separation of two adjacent gratings for the  $i$ th line is given by

$$\Delta L_i = 2^{i-1} \Delta L_1 \quad (2)$$

where  $\Delta L_1$  is the minimum separation between two gratings in line 1. Using Eq.(2) the time delay provided by the  $i$ th line can be written as

$$\tau_i = \frac{2 n_{eff} \Delta L_i}{c} \quad (3)$$

where  $n_{eff}$  is the effective refraction index of the fiber and  $c$  is the speed of light. Each of the  $2^N$  delay configurations of the PDM is an integer multiple,  $m$ , of

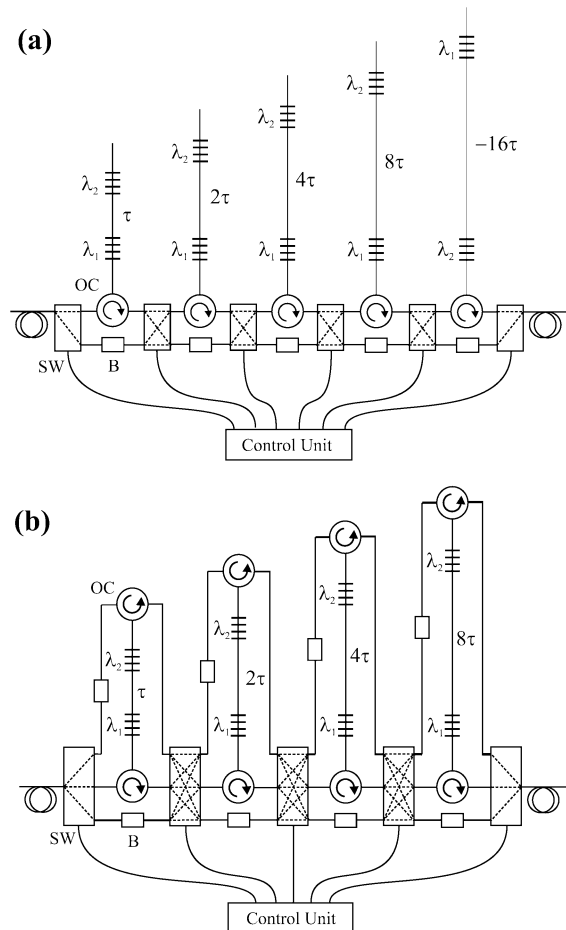


**Fig. 2** Two-channel 5-bit programmable dispersion matrix for: (a) Binary switching configuration; (b) Ternary switching configuration. SW: optical switch, B: optical balancer, OC: optical circulator.

minimum time delay  $\tau_1$ . The minimum time delay, associated with line 1, is directly related with the angular resolution and the minimum steering angle of any beamformer [5]. The steered angle  $\theta_m$  is related to a characteristic parameter of the PDM, that is  $\tau_1$ , and a geometrical parameter of the antenna, the T/R element spacing  $\Lambda$ , by

$$\theta_m = \arcsin \left( \frac{c m \tau_1}{\Lambda} \right) \quad (4)$$

As can be noted in Fig. 2(a), the order of FBGs in the last line is reversed. This inversion allows an almost symmetrical beamforming by obtaining time delays of opposite sign when the last line is combined with the others.

Time delays with opposite sign can also be achieved by routing the optical signal to the top end of a delay line. In the ternary PDM version shown in Fig. 2(b) this approach is used to obtain symmetrically distributed delay configurations.

The architecture of four delay-lines ternary-PDM is shown in Fig. 2. The PDM is arranged in a ternary

layout, so that, the RF signal modulating  $\lambda_1$  can either leads or lags the RF signal modulating  $\lambda_2$  in each line hence allowing perfect symmetrical beamforming. As we discussed above, to achieve the same resolution in binary systems an additional line is required. The  $2^N - 1$  delay configurations version of the two-channel ternary architecture consists of an array of  $N - 1$  delay lines. Each delay line is constructed in the same way as described for the binary case. Each possible time-delay can be calculated from

$$\tau(m) = \sum_{i=1}^{N-1} a_{i,m} \cdot \tau_i, \quad (5)$$

where the value of the constant  $a_{i,m}$  depends on the optical signal path. The optical signal can be routed to the bottom end or top end of the  $i$ th delay-line being  $a_{i,m} = 1$  and  $a_{i,m} = -1$  respectively. On other hand, when light is bypassing the  $i$ th delay line  $a_{i,m} = 0$ . Time-delays, which are integer multiples of the minimum delay  $\tau_1$ , range from  $-2^{N-1} \cdot \tau_1$  to  $2^{N-1} \cdot \tau_1$ . This results in a symmetrical distribution around zero delay. Because in the ternary arrangement the value for  $a_i$  is not unique for a certain time-delay  $\tau(m)$ . This property can be used to improve the performance of the system, i.e., a desirable time delay (a combination of array lines) is chosen by including a minimum number of delay-lines in order to avoid excessive insertion loss.

### 3. Experiment and Results

Two 15 mW semiconductor lasers, Alcatel model A1905LMI; with wavelengths of 1551.7 nm and 1550.9 nm provide optical carriers. Two in-fiber polarization controllers set proper polarization at the input of the 10 GHz bandwidth SDL EOMs. Experiments are performed over both, a 5-bit binary PDM that provide 32 delay configurations and a ternary PDM allowing 31 different delays. The central wavelengths of the fiber Bragg gratings match ITU frequency channels 32 and 33 (100 GHz spacing). All the gratings have reflectivity from 94.8% to 99.3% and FWHM of 0.3nm. For lines 1 to 4 the first FBG reflects light of channel ITU 32 meanwhile the second FBG reflects light of channel ITU 33. According to Fig. 2(a) the order of FBGs for line 5, in the binary version, is reversed in order to obtain symmetrical beamforming.

The minimum separation between FBG is  $\Delta L_1 = 0.02$  m corresponding to the line 1. Separations for successive lines are:  $\Delta L = 0.04$  m, 0.08 m, 0.16 m, and 0.32 m. The theoretical minimum time delay of the PDM, calculated from Eq. (2), is  $\tau_1 = 195.8$  ps. Optical circulators are used to route the signals to/from the lines. In the binary version, two  $1 \times 2$  and four  $2 \times 2$  Hitachi optical switches are programmed in order to obtain all the delay configurations. For the ternary system, two  $1 \times 3$  and three  $3 \times 3$  Hitachi optical switches

are used. In both approaches, optical switches are controlled using an Agilent 34970A data acquisition unit. Note that the optical signals will undergo different levels of attenuation depending upon the delay configuration, because the number of components is not the same for each of the paths. Thus, as the insertion loss of PDM is path dependent, spurious power variations from changes in constants  $K_1$  and  $K_2$  for different configurations can affect the measurements. In order to balance the optical power in the PDMs, in-fiber air-gap mechanical attenuators are placed in each of the paths as shown in Fig. 2(a) and (b). Optical insertion loss of the system is approximately 26 dB. The main sources of loss are the EOM biased on quadrature (6–8 dB) and the optical connectors along the PDM. Due to optical losses over the system, an IPG Photonics erbium doped fiber amplifier (EDFA) with 25 dB gain is inserted to improve the dynamic range of the network.

#### 3.1 Time-Delay Characterization

In order to characterize the delay-lines a slightly modified version of the setup shown in Fig. 1(a) is used. The modulator is fed with an RF signal out of port #1 of a Vector Network Analyzer. Port #2 detects the RF signal out of the two broadband photodetectors one at a time. Therefore, the phase and magnitude of S-parameter  $S_{21}$  are measured for each channel. For a given frequency, the time-delay introduced by the PDM can be obtained by subtracting the phase values associated with the parameter  $S_{21}$  for the two channels as

$$\Delta\phi_m = \phi_0 + 2\pi\nu_{RF}\tau(m), \quad (6)$$

where  $\Delta\phi_m$  is the phase difference for the  $m$ th delay configuration,  $\nu_{RF}$  is the signal frequency, and  $\phi_0$  is an arbitrary constant phase. Figure 3(a) shows the phase difference between channels for switching configurations involving: no delay and individual delay lines 1 to 5 of binary PDM. The experimental data is obtained by sweeping the RF signal from the vector network analyzer from 130 MHz to 2 GHz. The time delay is calculated from the linear fit to data using Eq. (6). Figure 3(b) shows the time-delays for all possible configurations of the PDM. The minimum time-delay corresponding to line 1 is calculated to be 219.3 ps. The linear behavior of the curve shows a good agreement with Eq. (6). Measurement errors are less than 10% and are attributed to grating spacing errors and phase noise.

#### 3.2 Beampattern Characterization in Transmit Mode

The results in this section characterize the array-factor, which is equivalent to the beampattern when isotropic antenna elements are used. For transmit mode characterization, the configuration shown in Fig. 1(a) is modified. The output signal from the PDM is detected by

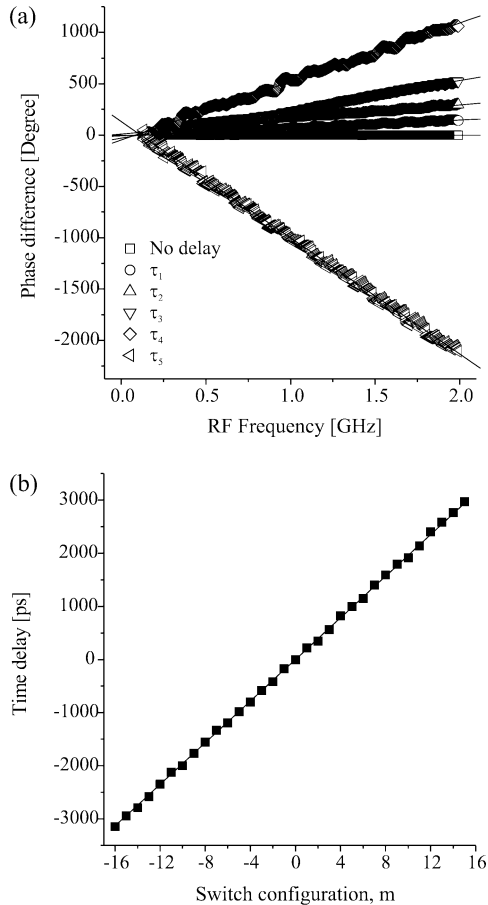


**Fig. 3** (a) Phase difference vs. RF frequency for: no delay and delay lines 1–5. (b) Time delay versus switch configuration (parameter  $m$ ) for all the possible time-delays in PDM.

a single photodetector and a Tektronix 2782 RF Spectrum Analyzer. Thus, the RF phase shift created by the PDM is transformed to power variations, according to Eq. (1). In order to obtain the transmit beam pattern for a desired RF frequency, the PDM is stepped through each possible time-delay configuration. Figure 4 shows the experimental and theoretical beam patterns for the transmission of a RF signal at 1 GHz. Plotted data represents power received by an observer at broadside position for different configurations of the PDM. The theoretical curve is calculated from Eqs. (1), (4) and (6). The plot represents a beam steering range of  $\pm 61.7^\circ$ , using  $\Lambda = 1$  m as the element spacing of the antenna-array. Discrepancies between the experimental points and the theoretical curves are attributed to errors in the power balance of the PDM and power fluctuations due to crosstalk. The bandwidth of the FBG for both channels causes some overlap between the reflectivity profiles, which in turn produces crosstalk.

### 3.3 Receive Mode Beam-Pattern Characterization

An HP model 83650A RF synthesizer simulates an in-

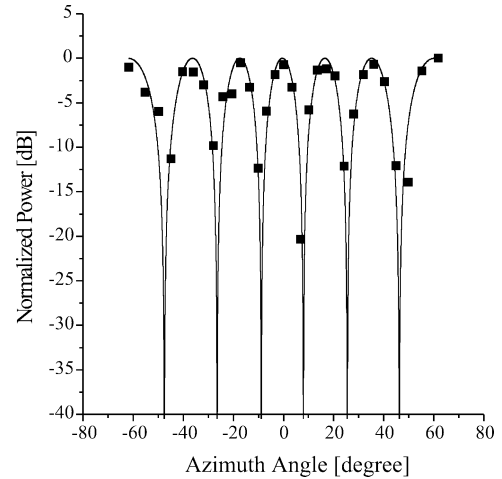


**Fig. 4** Beampattern obtained in transmit mode using the ternary PDM with 31 time-delay configurations. The frequency of the transmitted signal is 1 GHz.

coming RF signal from a target. The output of the RF synthesizer is split and sent to optical modulators shown in Fig. 1(b). To simulate the phase difference between two antenna elements due to a moving target an RF phase shifter is introduced before one of the modulators. Beam patterns are obtained by sweeping the RF phase shifter and measuring the RF output power from a single photodetector using a Tektronix 2782 RF spectrum analyzer.

Beampatterns are measured for RF signals in 0.2–0.8 GHz frequency range. Figure 5 shows beampattern measurements for three RF signals at 0.2, 0.5 and 0.8 GHz. Figure 5(a) correspond to zero delay, that is, the optical carriers do not pass through any of the FBG lines. Hence, a target is detected at the broadside position. For the measurement shown in Fig. 5(b) the carriers pass through the 4th delay line to provide a time-delay of  $8\tau_1$ .

In this case, the PDM is programmed for detecting a target at angular position of  $28.02^\circ$ . For all the above figures, experimental data are fit to Eqs. (1), (4) and (6). Notice that the antenna steering-angle is independent of the signal frequency. The position of the main lobe in Fig. 5 is shown to be the same for all three frequencies 0.2, 0.5 and 0.8 GHz thus demonstrating a “squint-free” characteristic of the processor. Figure 6 further demonstrates the “squint free” nature of the system. Here, dotted lines for several PDM configurations show the theoretical main lobe positions. The selected azimuth angles are  $-28.02^\circ$ ,  $0^\circ$ ,  $3.37^\circ$ ,  $6.74^\circ$ ,  $10.146^\circ$  and  $28.02^\circ$ . These angular positions in Fig. 3 correspond to values of parameter  $m = -8, 0, 1, 2, 3,$  and  $8$  respectively. Experimental data points are shown for 0.2, 0.5 and 0.8 GHz. Values for azimuth angles are obtained by fitting the theoretical curve to experimental results of beampatterns using a non-linear fit routine. In order to compare the performance of the

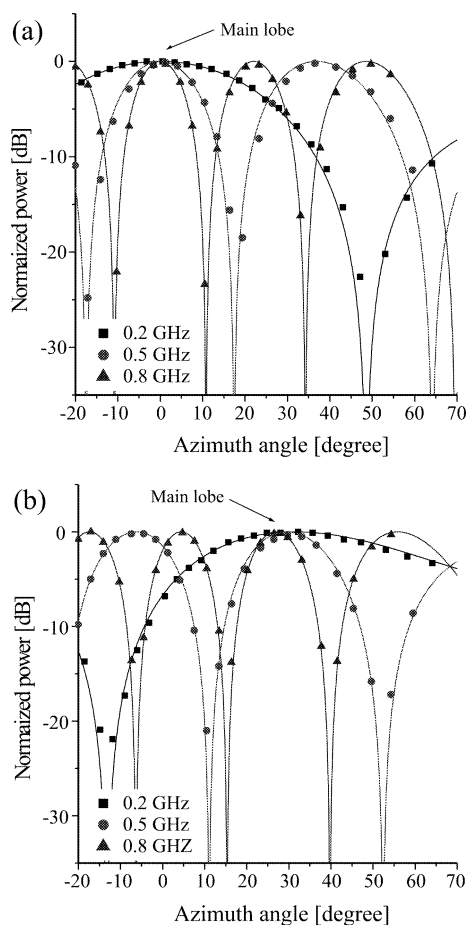


**Fig. 5** Beam patterns measurement for receive mode at 0.2, 0.5 and 0.8 GHz signal frequencies for target at azimuth angular position of: (a)  $0^\circ$  (broadside), (b)  $28.02^\circ$ . The main-lobe angular position is independent of RF operating frequencies. This shows the squint-free characteristic of this system.

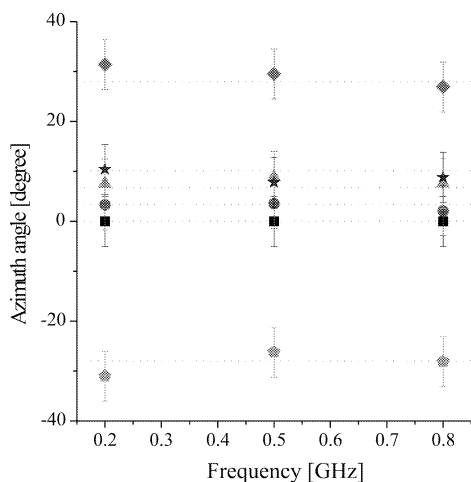


**Fig. 6** Comparison of azimuth angular positions of beam patterns in receive mode at RF values of 0.2, 0.5 and 0.8 GHz. Dotted lines represent theoretical values.

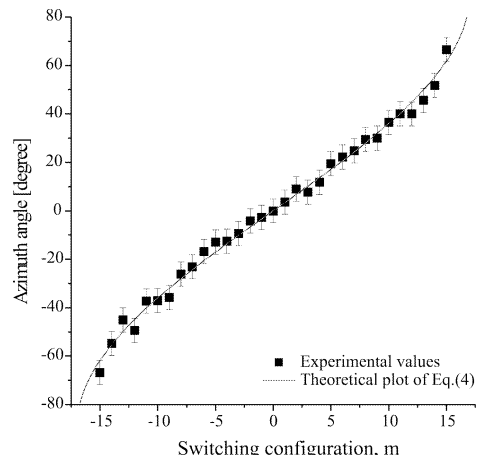


**Fig. 7** Azimuth position of the main lobe of the beam pattern for a received signal of 0.5 GHz. Solid line represents theoretical values of Eq. (3).

processor against theoretical predictions from Eq. (4), beam patterns for all time-delay configurations are measured. Figure 7 shows the azimuth angular position for the main lobe obtained from beam patterns at 0.5 GHz plotted against the switching parameter  $m$ . This figure shows a good agreement between fitted values and theoretical calculations.

Our measurements are limited to 0.8 GHz in order to obtain a reasonable number of data points per beam lobe. Otherwise, the upper limit is restricted by our phase-shifter and photodetector, which have a bandwidth of 2 GHz.

#### 4. Discussion and Conclusions

In conclusion, we have analyzed and characterized a 2-channel 5-bit optical beamformer system operating at 1550 nm using a binary and ternary PDM. Although only measurements performed over a ternary PDM are presented, equivalent performance is achieved for the binary version [6].

The working prototype is used to demonstrate time-delay measurements and beam pattern measurements in the transmit/receive mode for signals in 0.2–1 GHz frequency range. Beam patterns are obtained for steering angles of approximately  $\pm 62^\circ$ . Our optical beamformer exhibits squint-free behavior in RF band of 0.2–0.8 GHz.

Notice that no additional optical components such as, circulators, attenuators, or optical switches will be necessary in order to scale the binary and ternary PDM for phased-array antennas with a large number of elements. This upgrade will only require that more FBG to be added to each delay line. However, the ternary PDM requires one less delay line of FBG in order to obtain similar performance as its binary counterpart. This advantage is critical when large number of FBG have to be fabricated in a single delay line.

The use of FBG and WDM architecture for constructing PDM for phased-array antennas can be extended to process multiple simultaneous RF beams. In such approach, optical interleavers along with fused fiber couplers make possible the separation of optical channels carrying different RF beams. A simple prototype for processing two independent simultaneous beams in a 3-bit 2-channel beamformer has been constructed and is currently under investigation. Its development and preliminary results will be presented elsewhere.

### Acknowledgments

The authors would like to thank Daniel Purdy of Office of Naval Research for his support of this project under the contract number N00014-00-1-0782.

### References

- [1] N. Riza, ed., Selected papers on photonic control systems for phased array antennas, SPIE Milestone Series, Washington, vol. MS 136, 1997.
- [2] R. Soref, "Fiber grating prism for true time delay beamsteering," *Fiber and Integrated optics*, vol.15, pp.325-333, 1996.
- [3] H. Zmuda, A. Soref, P. Payson, S. Johns, and E. Toughlian, "Photonic beamformer for phased array antennas using a fiber grating prism," *IEEE Photon. Technol. Lett.*, vol.9, pp.241-243, 1997.
- [4] D. Tong and M. Wu, "Transmit/receive module of multiwavelength optically controlled phased-array antennas," *IEEE Photon. Technol. Lett.*, vol.10, pp.1018-1020, 1998.
- [5] B. Black, A. Siahmakoun, L. Slaybaugh, J. Chestnut, and D. Thalen, "Component-level simulation of optical beamforming systems," *Proc. SPIE*, vol.4532, pp.494-499, 2001.
- [6] S. Palit, S. Granieri, A. Siahmakoun, and B. Black, "Binary and ternary architectures for a two-channel 5-bit optical receive beamformer," *Proc. International Topical Meeting on Microwave Photonics*, pp.273-276, Awaji, Japan, Nov. 2002.



**Sabarni Palit** received her B.E. degree in Electronics and Telecommunications Engineering, in 2000, from Cummins College of Engineering, University of Pune, India, and her M.S. degree in Electrical Engineering from Rose-Hulman Institute of Technology, IN, in 2003. Her interests are in the fields of RF photonics and embedded systems.



**Mark Jaeger** received his B.S. degree in Electrical Engineering from the University of Stuttgart, Germany, in 2000, and his M.S. degree in Applied Optics from the Rose-Hulman Institute of Technology in 2002. His research interests are in the area of RF photonics, optical A/D conversion and optical communication systems.



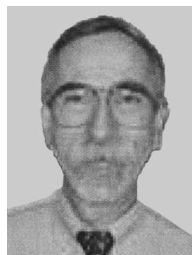
**Sergio Granieri** received the B.S. and Ph.D. degrees in physics from University of La Plata, Argentina, in 1993 and 1998, respectively. His doctoral research was concerned with the study and optical generation of the fractional Fourier transform and applications to signal processing. From 1994 to 1998, he worked at Optical Research Center (CIOP), La Plata, Argentina, where he has engaged in research on optical information processing.

From 1998 to 2000, he was assigned to the Optical Communication Laboratory (LAMECO) at the same institution, to pursue research on erbium-doped fiber amplifiers. Since 2000, he has been with Rose-Hulman Institute of Technology, Terre Haute, IN, where he has been principally involved with research on optical control of phased-array antennas for radar applications and optical analog/digital conversion.



**Azad Siahmakoun** received B.S., M.S., and Ph.D. in physics. He completed his doctoral degree at the University of Arkansas in 1987. He joined the department of Physics and Applied Optics of Rose-Hulman Institute of Technology in September of 1987 where he is now a professor of Physics & Optical Engineering and the director of Center for Applied Optics Studies. Dr. Siahmakoun has been active in optics education and research. He

has recently developed a microfabrication and MEMS laboratory for teaching undergraduate students. His research interests are in the area of applications of photorefractive crystals, RF photonics, optical analog-to-digital conversion and optical information processing.



**Bruce A. Black** completed his Ph.D. in engineering at the University of California at Berkeley. Since 1983 he has been on the faculty of the Department of Electrical and Computer Engineering at Rose-Hulman Institute of Technology in Terre Haute, Indiana, where he is also advisor to the Amateur Radio club (W9NAA). His interests are in communications, wireless systems, and signal processing.

**Jeffrey Chestnut** received B.S. degree in Electrical Engineering from Indiana University/Purdue University in 1984 and M.S. degree in Engineering Management from Rose-Hulman Institute of Technology in 1999. Since 1984, he has been a microwave/optics engineer at NSWC Crane. His interests are in the areas of RF Photonics and Radar design.